Mid-infrared Microspectroscopy of Difficult Samples Using Near-Field Photothermal Microspectroscopy

Azzedine Hammiche, Laurent Bozec, Matt J. German, John M. Chalmers, Neil J. Everall, Graham Poulter, Mike Reading, Dave B. Grandy, Francis L. Martin, and Hubert M. Pollock

The authors discuss progress in near-field IR microspectroscopy using a photothermal probe and show how it can be applied to the spectroscopic characterization of real-world samples.

Despite recent advances in Fourier transform-infrared (FT-IR) microspectroscopy and micro-attenuated total reflectance (ATR), for many types of samples there remains a need for even higher spatial resolution, or for a nondestructive method of recording localized mid-IR spectra from as-received samples without the risk of damage or alteration by preparation techniques. A promising technique is the recently developed method of near-field IR microspectroscopy using a photothermal probe. We discuss progress in the development of this technique and give examples of how it can be applied to the spectroscopic characterization of real-world samples.

Following a brief survey of several limitations of the more commonly used mid-IR microspectroscopy sampling techniques, this article briefly discusses the variants of near-field scanning probe methods, in which lateral spatial resolution is not subject to the diffraction limit, and which have been adapted to yield spectroscopic data in the mid-IR region. We then focus our discussions on the photothermal technique, and describe its use in characterizing and mapping the composition of a range of different samples. The goal, which has not yet been achieved, is true IR imaging, with spatial resolution at the tens of nanometers level; at present, the spectral detail is sensitive to changes as small as 2 µm in the positioning of the probe.

Existing Mid-IR Microspectroscopic Techniques (1)

Methods that combine microscopy with spectroscopy have been an important step forward in the analysis of complex inhomogeneous samples because any particular feature identifiable in a microscope image can be selected for localized spectroscopic analysis. Among the microoptical techniques, FT-IR microspectroscopy has a prime position within many industrial laboratories. Modes of operation include transmission, ATR mode, or transflectance mode.

In FT-IR transmission microscopy, for a continuous sample such as an organic polymer film, the sample thickness typically must be 10 µm or less. This should enable a satisfactory fingerprint spectrum showing all the peak maxima in the spectrum to be recorded, in which the strongest bands have transmission minima in the region of 10–20%. The sample also should be of uniform thickness, and preferably nonscattering or at least minimally scat-

tering. Given these conditions, such a film commonly features interference fringes, appearing as a superimposed sinusoidal pattern in the spectrum. To record transmission spectra that are free from other optical artifacts, a common practice is to flatten samples such as fibers or powder particles so that the material being examined has a uniform thickness. This often is done in a compression cell. Such treatments can, of course, alter the properties such as crystallinity, polymorphic form, or molecular orientation.

In internal reflection infrared (ATR) spectroscopy, the surface of a sample is placed into intimate contact with a higher refractive index, infrared transparent internal reflection element, and its spectrum is recorded with infrared radiation that is incident through the reflection element at an angle greater than the critical angle. Compared with transmission spectra, the relative intensity of bands in ATR spectra increases with increasing wavelength. Anomalous dispersion sometimes can give rise to distorted band shapes, with bands appearing to have a somewhat first derivative–like appearance. The effect is related to the change of refractive index through an absorption band. Distortions are most apparent for strong bands and when operating at lower angles of incidence. A recently developed and convenient sampling technique, single-bounce micro-ATR, has become widely used. In this technique a small region of the sample is located and pressed onto the face of a small ATR element, commonly diamond.

In the transflectance mode, a thin layer of a sample is placed onto a reflecting substrate such as a gold mirror. The mid-IR radiation passes through the sample and is reflected back by the mirror surface, so that the radiation effectively has passed through the sample twice. These transflectance spectra have superimposed on them a weaker specular reflectance spectrum, which has the appearance of a first-derivative spectrum. Spectra also can be recorded in specular (front-surface) reflection mode from suitable samples (that is, smooth, optically thick materials) but the resultant spectra are heavily distorted and

PHOTOTHERMAL MICROSCOPY PROVIDES A NONDESTRUCTIVE MICROPROBE APPROACH TO MID-IR SPECTROSCOPY FOR A WIDE RANGE OF SAMPLE TYPES, WITH LITTLE OR NO NEED FOR SAMPLE PREPARATION.

must be treated (usually with a Kramers–Kronig transform) to separate the refractive index and absorption index components of the spectra.

The advent of focal plane array detectors has ensured that global imaging by FT-IR microspectroscopy has become an extremely valuable technique for the characterization of inhomogeneous samples. Nevertheless, the restrictions imposed by sample preparation requirements remain. Furthermore, there is the major problem of diffraction, which effectively imposes limits on the lateral spatial resolution: any sample area examined that is of the order of the interrogating wavelengths (approximately 10 μm) is likely to suffer from diffraction effects, which give rise to spectral distortion and incursion of spectral features attributable to material outside of the area being examined. Recent developments include FT-IR microspectroscopy using either synchrotron radiation as the infrared source, with its high brilliance, low divergence and small effective source size, or tunable free-electron lasers. These enable spectral information to be recorded at significantly improved spatial resolution. Despite these developments, extending infrared investigations to below the diffraction limit requires more specialized approaches, using, for example, one of the various types of scanning probes.

Existing Scanning Probe Approaches to Vibrational Spectroscopy

The generic term "scanning probe microscopy" (not to be confused with scanning electron microscopy) includes particular methods such as atomic force microscopy, scanning tunneling microscopy, and many other variants. The key feature of such scanning probe techniques is that they are not subject to the diffraction limit of spatial resolution. In traditional variants of microscopy, the spatial resolution depends upon wavelength, as determined by the relevant classical theory (more precisely, far-field optics, where the resolution is limited by diffraction). In contrast, the scanning probe methods in general are near-field techniques, and the spatial resolution is dominated by other factors, such as probe size. Until recently, most attempts to apply scanning probe technology to localized spectroscopy have employed UV/Vis absorption or photoluminescence to provide the signal that determines the contrast in the microscope image. The past few years have seen efforts to harness the analytical power of IR spectroscopy and Raman scattering. Östershultze and colleagues (2), Dragnea and Leone (3), and Pollock and Smith (4) provide reviews of these topics. In scanning near-field optical microscopy, to achieve the near-field criterion, the light source must be smaller than the optical wavelength. Examples of such a source are an aperture such as the tip of a tapered optical fiber, or a minute object

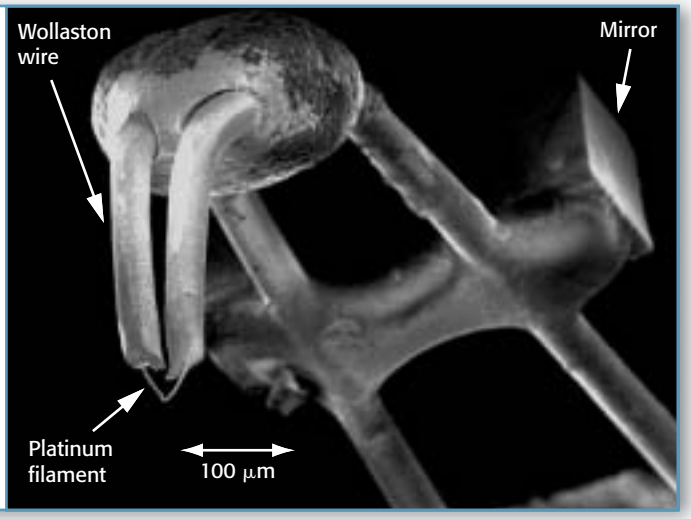

Figure 1. Wollaston thermal probe (28). The temperature is sensed by the apex of a V-shaped 5-mm diameter platinum–10% rhodium wire (after reference 29, copyright 2001, with permission from Elsevier Science). See also references 26 and 30.

that acts as a light-scattering source (also known as aperturless scanning near-field optical microscopy). These two approaches can achieve spatial resolution in the range of 10–100 nm.

For mid-IR scanning near-field optical microscopy, low signal levels pose problems. There are difficulties in preparing high-throughput fibers for use in the mid-IR, especially at wavelengths greater than approximately 4 μm. In addition, photomultiplier tubes or avalanche photodiodes as detectors do not operate in the mid-IR region of the spectrum, and typical photoconductive detectors for mid-IR wavelengths are several orders of magnitude less sensitive than they are in the visible. Several groups have concluded that once again, the aperturless probe offers a more attractive approach (5–7). A cantilevered metal wire probe or a metallized atomic force microscope probe, acting as a scatterer of the signal from the sample, is placed at a distance from the sample that is less than the wavelength of the light (near-field scattering). The scattered signal is detected using far-field optics. In addition, recent technical developments have allowed sub-wavelength Raman mapping using near-field probes to be achieved (8–9). A Raman imaging spectrometer is integrated with a scanning near-field optical microscopy based on either an extruded optical fiber or a scattering center such as a colloidal noble metal surface.

Near-Field Photothermal IR Microspectroscopy (PTMS)

At the heart of this technique (10) is a special version of the type of probe used in atomic force microscopy (AFM): the scanning thermal probe. This is a miniature thermometer, and originally was developed to serve the version of AFM known as scanning thermal microscopy (11). As in scanning thermal microscopy, the photothermal instrument generally uses an "active" thermal probe as a heater as well as a thermometer (Figure 1). It can give multiple images of the sample whose contrast reveals surface topography as well as sub-surface detail that results from local variations in the thermal conductivity of the sample. Again, as in other scanning probe methods, these images are not subject to the diffraction limit of spatial resolution.

Thus, given its ability to provide spectral data (as explained below), the instrument in principle can be operated in either of two modes: the mapping mode, in which IR spectra are obtained from individual regions selected from the scanning thermal microscopy image; and the IR imaging mode, in which an image is obtained whose contrast is determined by the local concentration of material that absorbs in a given band of the spectrum. To date, data from the IR imaging mode are as yet unpublished.

A related development of scanning thermal microscopy is micro-thermal analysis (12, 13), in which the AFM images are used to select individual regions of the sample, which then are fingerprinted or analyzed by localized thermomechanometry, calorimetry, or analytical pyrolysis. In all cases the same thermal probe is used as with the photothermal technique; thus a single instrument could be used to probe a range of material properties, including chemical, morphological and physical properties, from precisely the same area of the sample. The ability to record IR data that can be related directly to complementary images and microthermal analyses would be a boon to researchers, and has been shown to be possible for composite samples of acrylic resin–polyethylene terephthalate (14). Thermal conductivity mapping, localized thermomechanical analysis, and IR spectra were obtained from individual regions. Other advantages of the

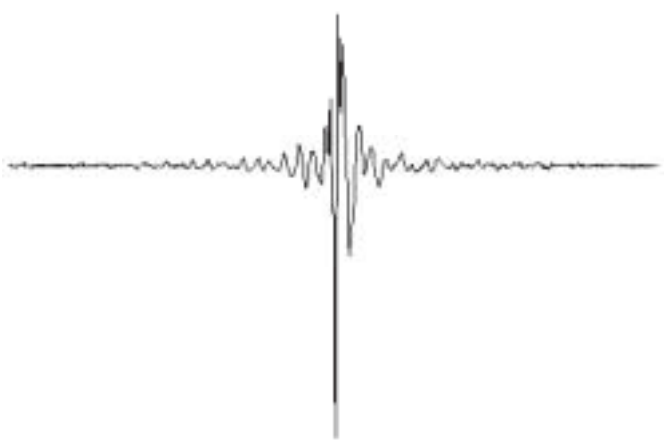

Figure 2. Photothermal interferogram. The maximum signal-to-noise ratio achieved to date was obtained using the experimental probe being developed by T.A. Instruments (30), as in the single-pass background interferogram shown here (no coaddition was used).

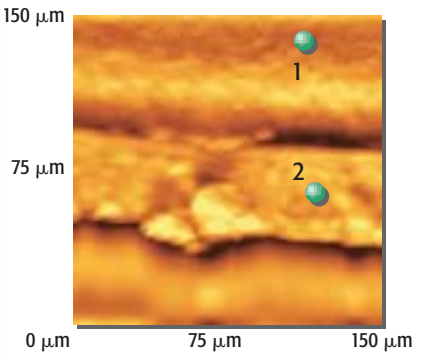

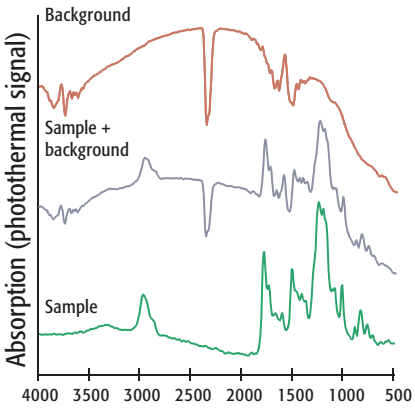

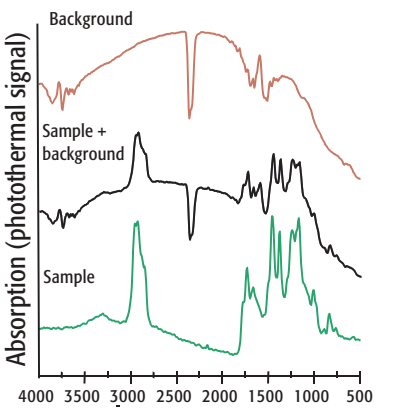

Figure 3. Analysis of a composite polymer sample consisting of a thin film of polymer X sandwiched between two slabs of polymer Y. Top: topographic AFM image. Bottom: The spectra labeled "Sample + background" are derived from data obtained at points shown on the image as 1 and 2. Subtraction of the background spectrum then gives the spectra that characterize these regions of the sample. Experimental parameters are described in the text.

photothermal technique include the potential for circumventing diffraction problems associated with FT-IR microscopy, as mentioned earlier, and hence obtaining better lateral spatial resolution information. Here we show that even without particularly high spatial resolution, PTMS can be viewed as a convenient, nondestructive, direct (maybe even noncontact) sampling technique that allows for direct sampling of materials of awkward geometry, such as fibers or hair. Another potential application is single-particle analysis without the need of sample preparation. Clearly, there are situations when the advantage of doing no sample preparation on a sample is of high value to avoid effects such as pressure-induced polymorphic changes.

Instrumentation. If a sample absorbs IR radiation it heats up. When an intensity-modulated beam supplied by a conventional FT-IR spectrometer is used, the measured temperature of the sample fluctuates accordingly. This temperature is measured, as a function of time, by the scanning thermal probe in passive mode, in which it acts simply as a thermometer. Its output signal is amplified and fed into the external input of the same spectrometer, thus providing an interferogram (Figure 2), which replaces the interferogram normally obtained by means of direct detection of the IR radiation transmitted or reflected by the sample. The Fourier transform algorithm is performed on this interferogram after digitization, in the normal way, to give the spectrum.

To perform this procedure as a function of location on the sample surface, the probe is mounted on a simple positioning system, or, if images are required, in an atomic force microscope. In either case an appropriate optical interface is required to direct the spectrometer's external infrared beam onto the sample and to increase the flux at the sample surface and increase the signal-to-noise ratio. The IR beam is focused to a spot 2 mm in diameter. Probe and sample surface are brought into contact at the focal point. As an alternative, we have constructed a dedicated AFM designed to fit directly inside the sample chamber of most FT-IR spectrometers.

Proof of concept. Proof of concept of PTMS has been detailed in earlier publications (10, 15). These describe how, for a number of polymers, prominent absorption peaks are resolved clearly and correlate well with those contained in a conventional ATR spectrum obtained from the same material, and that the overall shape of the main peaks or bands reflects the fact that the spectrum is a convolution of different contributions from both optical and thermal properties. Furthermore, tests on a model bilayer system have confirmed the feasibility of subsurface detection of polymers; a "nanosampling" version of the technique is possible (14), in which the sample material is deliberately made to contaminate the tip, which then is lifted away so that the contaminant can be analyzed by PTMS. A complementary technique also has been developed that uses tunable monochromatic radiation. An optical parametric generator is used as the infrared source. Experiments have been performed using a synchrotron radiation source giving greatly improved spectral contrast (15).

Examples of Data Obtainable By PTMS

Figures 3–9 show different types of data that can be obtained using PTMS. Except where otherwise indicated in figure captions, the following equipment and conditions were used: The sample was positioned using a simple *xyz* translation stage. AFM imaging was accomplished using a Veeco (Woodbury, NY) Explorer scanning probe microscope. A Wollaston-type thermal probe (Figure 1) positioned at the IR focal point was used as the detector. The spectrometer was a Bruker (Billerica, MA) Vector 22 FTIR. We used a custom-built optical interface and preamplifier obtained from Specac Ltd. (Smyra, GA) and a Stanford Research (Sunnyvale, CA) model SR650 filter amplifier with the gain set to 100 dB. The mirror speed was 2.2 kHz, the spectral resolution was 16 cm^{-1}, and the number of co-additions was 2000.

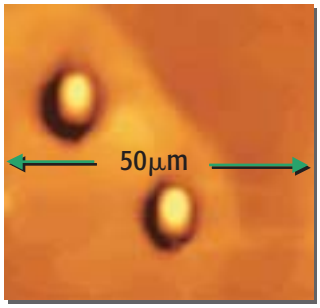

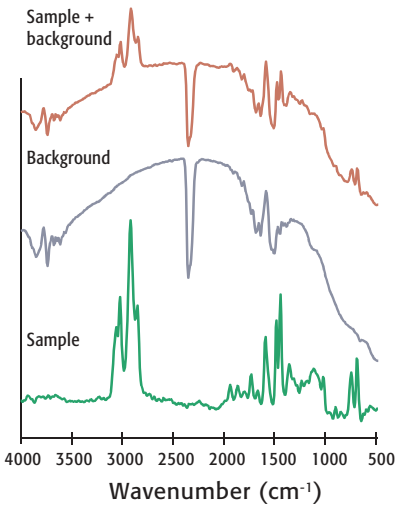

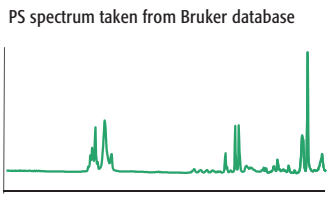

Figure 4. Analysis of microspheres from a polystyrene powder sample. The particles, which had nominal diameters of 5 μm, were spread and embedded into the surface of a rock salt window. The AFM image was obtained using a standard Si_3N_4 probe. Spectra are labeled as in Figure 3. For comparison, the fourth spectrum (polystyrene reference) is taken from the database of Bruker UK. Experimental parameters as given in the text, but with 4000 coadditions.

First, various model samples have been used to assess the performance of the technique. A sandwich of two polymers is shown in Figure 3, where the junction is seen in cross-section, together with IR spectra obtained from regions on opposite sides of the junction. If we choose a region of polymer A that is closer to the junction than some minimum distance, typically approximately 5–10 μm, then as a result of thermal diffusion, the spectrum obtained will be contaminated by peaks characteristic of material B. Therefore, with this probe and modulation frequency, the lateral resolution, as determined by thermal diffusion, is similar to the diffraction limit of a conventional FT-IR microscope. As is described elsewhere (16), the data subsequently might be processed by a weighted subtraction of the B spectrum, if this is already known, to isolate the spectrum of A. If not, the nanosampling technique, which avoids the thermal contamination problem, can be used to provide the B spectrum.

On a more applied theme, of obvious interest is the question of the smallest quantity of a given material that will yield useful spectral data. We examined a powder sample consisting of polystyrene spheres 5 μm in diameter: Figure 4 shows a recognizable spectrum of polystyrene obtained from a cluster of, at most, two of these spheres. Another example of data obtained from a powder sample is described in reference 15. Spectra have been obtained from samples of even smaller volume by means of nanosampling, as shown in Figure 5. We conclude that if a particle is either isolated or surrounded by IR-transparent material, extremely small amounts of material can be analyzed.

Earlier, we outlined how the probe is positioned onto a selected region of the sample using the AFM procedure, which includes the use of force feedback to control the final approach of probe to surface. Alternatively, an optical microscope can be incorporated into the instrumentation, and accurate positioning still is possible without the use of force feedback, as shown in Figure 6. This shows an image of the side of a human hair, together with the corresponding IR spectrum. (As yet, the setup is not well purged and hence some intrusion of water vapor bands into the spectrum is evident.) In the thermal contrast image (scanning thermal microscopy mode), the probe is operated as a heat source whose temperature is maintained constant as it is scanned. This results in the mapping of heat flow out of the probe, and the contrast mainly is due to thermal conductivity variation (that of the hair and that of the surrounding air). We see that the probe can be used in a simple scanning system to obtain images of the sample surface, thus permitting positioning of the probe without the need for a complex optical detection scheme for topography mapping. The figure shows also another example of data obtained from a sample with awkward geometry, namely a copper filament coated with a polymeric material.

Turning to other practical applications, there must be a wide range of samples from which useful spectral data can be obtained from tests that require no precise lateral positioning. Here, no microscope is needed, although clearly it still is necessary to have a means of controlling the vertical approach of the probe. Moreover, the sample need not consist of solid material. We have shown elsewhere (15) that even though water absorbs strongly in the mid-IR, a solution of a surfactant in microdroplet form gives a recognizable spectrum. There is of course no obstacle to analyzing a small quantity of solution once it has dried, such as a contaminant on a wipe. In one experiment, when a drop of a solution of a binary polymer blend in toluene was spilled on the laboratory bench and mopped up with paper tissue, we obtained spectra consistent with that of polystyrene.

There is increasing interest in the potential application of FT-IR spectroscopy as a diagnostic tool for diseases such as cancer (17, 18). The rationale for this approach is that vibrational spectra from normal cells will provide a particular biochemical finger-

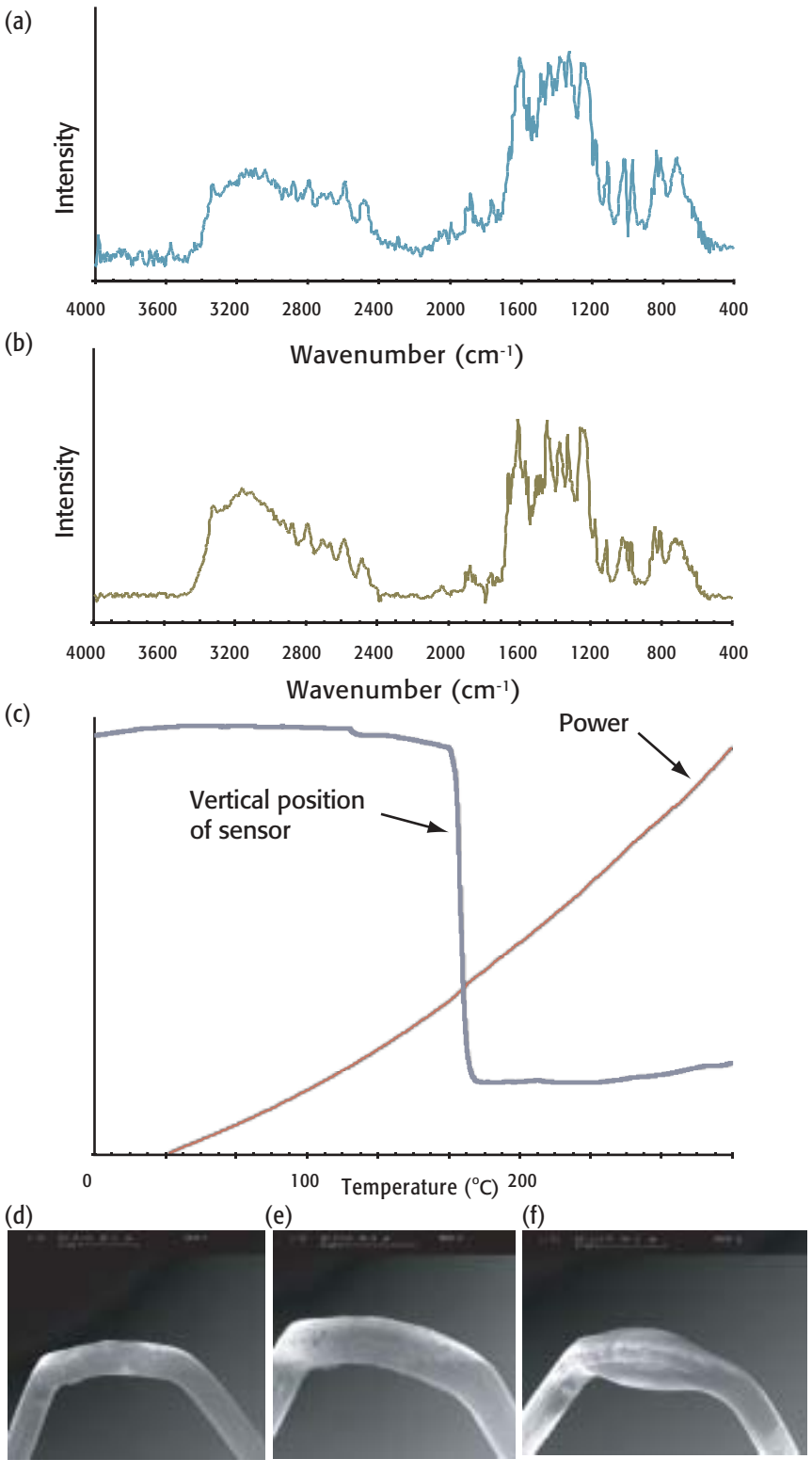

Figure 5. FT-IR nanosampling of paracetamol: (a) nanosample (1.6 kHz, 5 min, 8 cm^{-1} spectral resolution); (b) standard contact spectrum (1.6 kHz, 15 min, 8 cm^{-1} spectral resolution). (c) The micro-thermal analysis data are consistent with the known melting point of paracetamol. (d) The clean probe. (e) After micro-thermal analysis, the molten material has resolidified. The mass of material analyzed can be estimated to lie in the picogram to femtogram range. (f) A larger volume, in the nanogram range.

print and that, in comparison, analysis of cells from diseased tissue will give rise to spectral differences. It also has been hypothesized that FT-IR spectral-derived estimations of intracellular metabolites such as phosphate, glycogen, RNA, and DNA could be gainfully employed to differentiate normal versus malignant cells (17, 18). Of course, the potential applications of FT-IR microspectroscopy are wide ranging and include studies into pericellular proteolysis (19), antioxidant-induced changes in oxidized DNA (20), and the structure and conformation of proteins (21).

This leads to questions regarding sensitivity requirements: whether a relatively insensitive probe is required that gives an averaged spectrum of the multiplicity of intracellular workings, or whether even greater sensitivity is required to isolate specific chemical interactions. An analysis of populations of cells from normal versus malignant tissues, while clearly giving rise to spectral differences (18), could be a somewhat crude approach because of dilution effects. For instance, a biopsy sample of neoplastic tissue might contain only 2% malignant cells and also, normal adjacent tissue could well still contain a few transformed cells. Hence relatively small spectral changes heavily dependent on chance would be generated. A better approach is to analyze single cells by FT-IR spectroscopy and then examine them retrospectively for characteristic morphological changes (17). Such an approach would result in biochemical fingerprints based upon vibrational spectra characteristic of normal cells of particular origin: spectral deviations then would point to the presence of abnormal cells. This approach bypasses problems associated with the examination of cell populations that might contain cells in different phases of growth (cell cycle) or death (apoptosis). However, it does not bypass the needle-in-a-haystack problem; that is, the fact that a cell can be looked upon as a world unto itself with reactions and interactions continually ongoing in an intracellular galaxy of microenvironments.

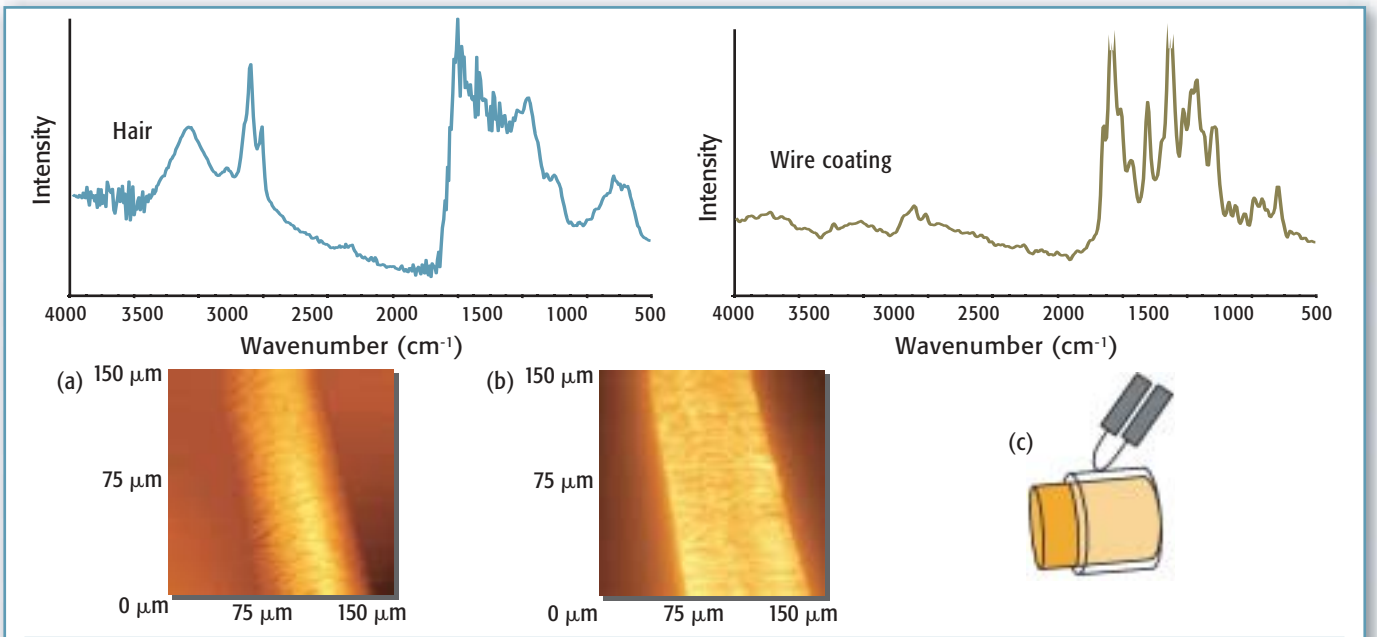

Figure 6. Analysis of samples with awkward geometry. Left spectrum: Fine strand of human hair, 120 μm in diameter; (a) topography image, obtained from the photodetector feedback signal, without the use of force feedback; (b) thermal contrast image, probe operated as a heat source whose temperature is maintained constant as it is scanned. This results in the mapping of heat flow out of the probe. The contrast is due mainly to thermal conductivity variation. Right spectrum: a free-standing chromel wire (125 mm diameter) coated with a 3 μm thick polyimide film for insulation; (c) a schematic showing the PTMS probe in contact with the surface of the wire coating. The spectrum is consistent with that of polyimide, together with some surface contaminant material.

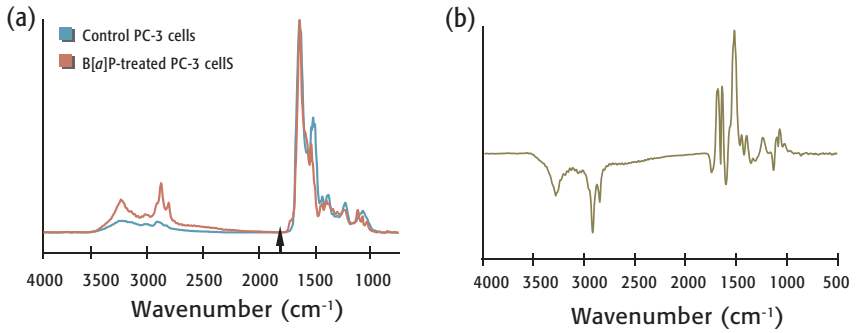

Figure 7. Characterization of malignant cells. The spectra show differences induced in whole cells following 24-h treatment with a chemical carcinogen, benzo[*a*]pyrene. Immortalized prostate (PC-3) cells were seeded as 3-mL aliquots (~ $1x10^4$ cells) into 30-mm petri dishes containing glass coverslips at 37 °C and 5% carbon dioxide. The cells were allowed 24 h to attach to the coverslips and then were treated with 1 μM benzo[*a*]pyrene (added as a stock solution in dimethyl sulfoxide, <1% v/v) for a further 24 h. The medium then was aspirated and the cells were washed with phosphate buffered saline before being fixed with 70% ethanol. Samples then were dehydrated under vacuum overnight before analysis. (a) Normalized spectrum of control PC-3 cells (blue line) and benzo[*a*]pyrene-treated PC-3 cells (red line); (b) the result of subtracting the spectrum from carcinogen-treated cells from the spectrum obtained for control PC-3 cells. Some bands of interest include the amide I peak at 1654 cm^{-1}, the amide II peak at 1545 cm^{-1}, the DNA peak at 1020 cm^{-1}, the RNA peak at 1121 cm^{-1}, the glucose peak at 1030 cm^{-1}, the phosphate peak at 1080 cm^{-1}, and the phospholipids peak at 2924 cm^{-1}.

Figure 7 shows PTMS spectra we have obtained from control and benzo[*a*]pyrene-treated prostate (PC-3) cells. In accordance with previously published studies (17, 18), characteristic vibrational spectra were obtained. (Nulling of the carbon dioxide absorption band at 2300 cm^{-1} was used to perform a weighted background subtraction. Note that airborne water vapor bands at ~4000–3500 cm^{-1} have also been eliminated from the spectrum on this occasion using this procedure.) Spectral differences in cells treated with benzo[*a*]pyrene as compared with control cells were observed. However, the question remains as to whether these spectral differences are just the consequence of an analysis of two different cells.

To illustrate the difficulty in isolating intracellular effects let us examine what occurs in this simple experiment. Benzo[*a*]pyrene is a lipophilic carcinogen that will readily cross cell membranes. Dependent upon a cell's

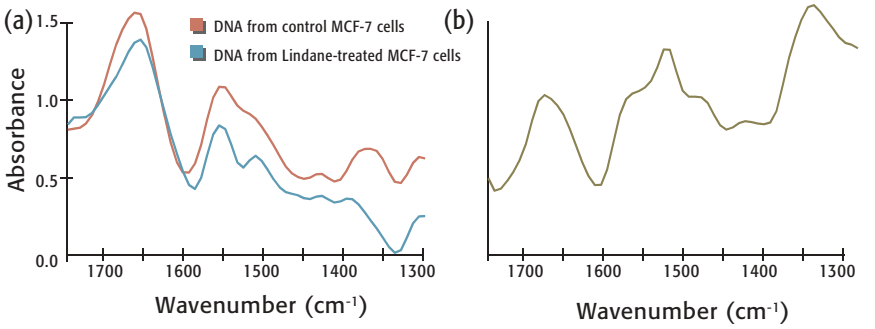

Figure 8. Damage to DNA induced by picomolar concentrations of lindane. The spectra show differences induced in isolated single-stranded DNA following a 24-h treatment with lindane of immortalized estrogen-receptor positive mammary (MCF-7) cells. Cells were treated for 24 h with 10^{-11} M lindane (added as a stock solution in dimethyl sulfoxide, < 1% v/v) before suspension in low-melting point agarose and application onto glass coverslips. After agarose was allowed to set on a cold surface, the cells were lysed at high pH to release individual cell genomes and denature double-stranded DNA into single strands. Following a DNA unwinding step, samples were dehydrated under vacuum overnight before analysis. (a) Normalized spectrum of DNA isolated from control MCF-7 cells (blue line) and lindane-treated MCF-7 cells (red line); (b) the result of subtracting the spectrum from lindane-treated cell DNA from the spectrum obtained for control MCF-7 cell DNA. Spectral vibrations between 1750 cm^{-1} and 1350 cm^{-1} are attributed to alterations in base structures, and comparisons of spectral properties in this region provide insights into alterations in the base and backbone structure of DNA.

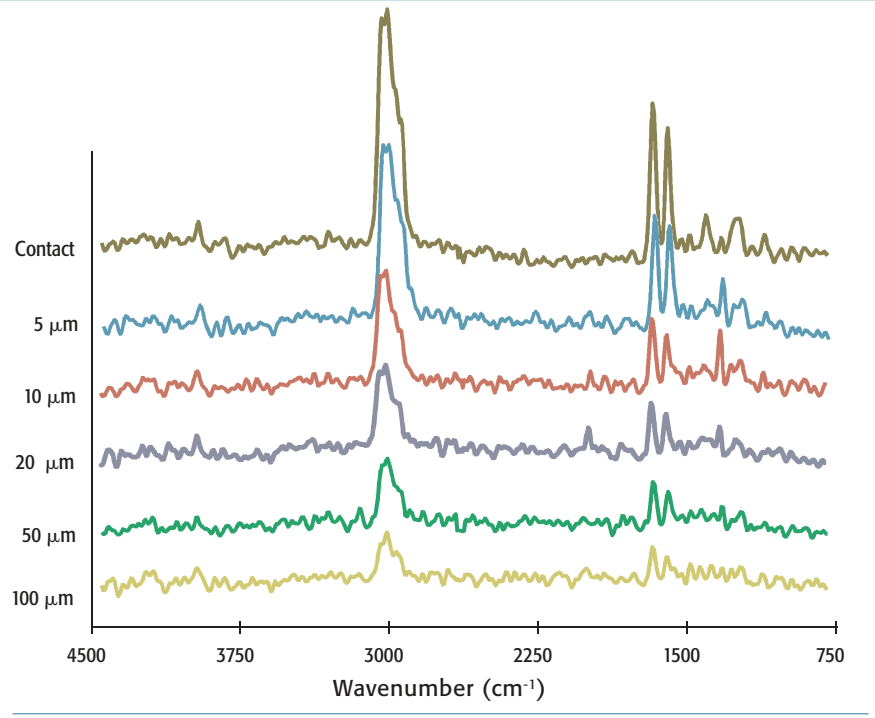

Figure 9. Noncontact spectra of polypropylene, illustrating heat transfer through air. The approximate distance of the probe from the sample surface is shown on the left.

ability to metabolically activate this carcinogen, benzo[*a*]pyrene is converted to a reactive electrophile that then binds covalently to nucleophilic sites in DNA to form bulky chemical DNA adducts. PC-3 cells contain this metabolic machinery. A human cell genome contains 3.12 billion bases and the concentration of benzo[*a*]pyrene used here results in 2–15 adducts per 10^8 nucleotides in prostate cells (22). While such adducts give rise to structural alterations, these are going to be relatively localized and the possibility of isolating such effects extremely random. To differentiate between a control and benzo[*a*]pyrene-treated cell, the average of how many spectral readings would be needed? Probably thousands, at the very least, would be required.

To address this question we examined spectral changes in DNA isolated from cells treated with picomolar concentrations of the organochlorine pesticide, lindane. Such agents are endocrine disruptors and increasingly are associated with the induction of low-dose effects (23). In this experiment isolated DNA was denatured into two single strands. Spectral vibrations between 1700 cm^{-1} and 1350 cm^{-1} are attributed to alterations in base structures associated with the induction of changes in conformational properties; these are markedly apparent in Figure 8. With increasing sensitivity of the methodology a correspondingly increasing simplicity of matrix is required: future experiments will involve the spectral characterization of carcinogen-modified oligodeoxynucleotide adducts (24).

It is likely that fine-scale PTMS measurements will provide key data for the study of a far larger range of samples than can be outlined here, ranging from a single powder particle of an illicit drug or a fragment of paint, to part of a painting in situ, the lubricant on a ball-bearing, or the variation in surface crystallinity along a stressed polymer molding. When necessary, spectra can be obtained without the need for direct contact between probe and sample (Figure 9).

Prospects For High Spatial Resolution in PTMS

Much already has been achieved with the PTMS approach, even without achieving higher spatial resolution. We have seen that the technique provides a novel, nondestructive microprobe approach to mid-IR spectroscopy, for a wide range of sample geometries and physical forms, and with little or no need for sample preparation.

We anticipate even greater success in the near future with improvements to our PTMS system. As outlined earlier (13), in other modes of imaging the same type of thermal probe can achieve submicrometer resolution. With PTMS, ultimately the spatial resolution will be limited simply by the size of the probe and the temperature distribution within the sample, rather than the infrared wavelength. Rather than diffraction being a limiting property to spatially resolving spectra, with PTMS the balance between the optical absorption and thermal diffusion lengths becomes critical. Various additional factors will affect the spatial resolution, including the size of the probe, the sharpness of the temperature distributions that result from the absorption of infrared energy by the inhomogeneities that are to be identified, and the finite heat capacity of the probe, which must perturb the temperature distributions to be detected. Further improvement in spatial resolution could be achieved by making use of the damped nature of thermal waves, such that the thermal diffusion length (25) can be made smaller than the probe size. In an as yet unpublished study we find that PTMS at a spatial resolution better than the diffraction limit may be achieved with the help of the smaller micromachined type of thermal probe (26), and elsewhere (27) we have discussed the prospects of achieving better than 1-µm resolution.

Acknowledgments

We thank the U.K. Engineering and Physical Sciences Research Council (EPSRC) and TA Instruments, Inc. (New Castle, DE), for financial support, ICI plc Measurement Science Group (Redcar, England) for a studentship, Bruker UK (Coventry, England) for the loan of equipment, and J Laveissière who obtained the nanosampling results.

References

1. J.M. Chalmers and P.R. Griffiths, Eds., *Handbook of Vibrational Spectroscopy* (John Wiley & Sons Ltd., Chichester, England, 2002).
2. E. Österschulze, M. Stopka, and R. Kassing, *Microelectron. Eng.* **24**, 107 (1994).
3. Dragnea and S.R. Leone, *International Reviews in Physical Chemistry* **20**, 59 (2001).
4. H.M. Pollock and D.A. Smith, in *Handbook of Vibrational Spectroscopy* (John Wiley & Sons Ltd, Chichester, England), vol. 2, pp. 1472–1492.
5. R. Bachelot, P. Gleyzes, and A.C. Boccara, *Opt. Lett.* **20**, 1924 (1995).
6. B. Knoll and F. Keilmann, *Nature* **399**, 134 (1999).
7. A. Piednoir, C. Licoppe, and F. Creuzet, *Opt. Comms.* **129**, 414 (1996).
8. D.A. Smith, S. Webster, M. Ayad, S.D.

Evans, D. Fogherty, and D.N. Batchelder, *Ultramicroscopy* **61**, 247 (1995).
9. Y. Narita, T.T. Ikeda, T. Saiki, S. Mononobe, and M. Ohtsu, *Appl. Spectrosc.* **52**, 1141 (1998).
10. A. Hammiche, H. M. Pollock, M. Reading, M. Claybourn, P. Turner, and K. Jewkes, *Applied Spectroscopy* **53**, 810–815 (1999).
11. A. Majumdar, *Ann. Rev. Mater. Sci.* **29**, 505 (1999).
12. D.M. Price, M. Reading, A. Hammiche, and H. M. Pollock, *International Journal of Pharmaceutics* **192**, 85–96 (1999).
13. H.M. Pollock and A. Hammiche, *J Phys D: Appl Phys* **34**, R23–R53 (2001).
14. M. Reading, D. Grandy, A. Hammiche, L. Bozec, and H.M. Pollock, *Vibrational Spectroscopy* **901**, 257–260 (2002).
15. L. Bozec, A. Hammiche, H. M. Pollock, M. Conroy, J. M. Chalmers, N. J. Everall, and L.Turin, *J Appl Phys* 90, 5159–5165 (2001).
16. L. Bozec, PhD Thesis, Lancaster University (2003).
17. M. A. Cohenford and B. Rigas, *Proc. Natl. Acad. Sci. USA* **95**(26), 15327–15332 (1998).
18. S. Argov, J. Ramesh, A. Salman, I. Sinelnikov, J. Goldstein, H. Guterman, and S. Mordechai, *J Biomed. Opt.* **7**(2), 248–254 (2002).
19. S. Federman, L.M. Miller and I. Sagi, *Matrix Biol.* **21**(7), 567–577 (2002).
20. D.C. Malins, K.E. Hellstrom, K.M. Anderson, P.M. Johnson, and M.A. Vinson, *Proc Natl Acad Sci USA* **99**(9), 5937-5941 (2002).
21. C. Vigano, E. Goormaghtigh, and J.M. Ruysschaert, *Chem. Phys. Lipids* **122**(1-2), 121–135 (2003).
22. F.L. Martin, K.J. Cole, G.H. Muir, G.G. Kooiman, J.A. Williams, R.A. Sherwood, P.L. Grover, and D.H. Phillips, *Prostate Cancer Prostatic Dis.* **5**(2), 96–104 (2002).
23. E. Yared, T.J. McMillan, and F.L. Martin, *Mutagenesis* **17**(4), 345–352 (2002).
24. K. Brown, C.A. Harvey, K.W. Turteltaub, and S.J. Shields, *J Mass. Spectrom.* **38**(1), 68–79 (2003).
25. D.P. Almond and P.M. Patel, *Photothermal Science and Techniques* (Chapman and Hall, London, 1996).
26. H. Zhou, A. Midha, G. Mills, S. Thoms, S.K. Murad, and J.M.R. Weaver, *J Vac. Sci. Technol.* **B16**, 54–58 (1998).
27. A. Hammiche, L. Bozec, M. Conroy, H.M. Pollock, G. Mills, J.M.R. Weaver, D.M. Price, M. Reading, D.J. Hourston, and M. Song, *Journal of Vacuum Science & Technology* **B18**(3), 1322–1332 (2000).
28. R.B. Dinwiddie, R.J. Pylkki and P.E. West, in *Thermal Conductivity* 22, T.W. Tong, Ed. (Technomics, Lancaster, USA, 1994), pp. 668–677.
29. P.G. Royall, D.G.M. Craig, and D.B. Grandy, *Thermochimica Acta* **380**(2), 165–173 (2001).
30. R. Dekhter, E. Khachatryan, Yu. Kokotov, and A. Lewis, *Appl Phys. Lett*. **77**, 4425–4427 (2000). ■

Azzedine Hammiche, Laurent Bozec, Matt J. German, and Hubert M. Pollock*
Department of Physics, Lancaster University, England
John M. Chalmers
School of Chemistry, University of Nottingham, and V S Consulting, England
Neil J. Everall
Measurement Science Group, ICI plc, England
Graham Poulter
Specac Ltd, England
Mike Reading and Dave B. Grandy
IPTME, Loughborough University, England
Francis L. Martin
Department of Biological Sciences, Lancaster University, England.

*To whom all correspondence should be addressed.
E-mail: h.m-pollock@lancaster.ac.uk.